Bioorganic & Medicinal Chemistry 23 (2015) 7150–7157

Contents lists available at ScienceDirect

Bioorganic & Medicinal Chemistry

journal homepage: www.elsevier.com/locate/bmc

# Targeted Shiga toxin–drug conjugates prepared via Cu-free click chemistry

Vesela Kostova, Estelle Dransart, Michel Azoulay, Laura Brulle, Siau-Kun Bai, Jean-Claude Florent, Ludger Johannes, Frédéric Schmidt *

*Institut Curie, CNRS, UMR 3666/INSERM U1143, 26 rue d'Ulm, 75248 Cedex 05 Paris, France*

ARTICLE INFO

*Article history:*
Received 21 July 2015
Revised 5 October 2015
Accepted 6 October 2015
Available online 8 October 2015

*Keywords:*
Targeted drug delivery
Shiga toxin
Copper-free click
Doxorubicin
Auristatin

ABSTRACT

The main drawback of the anticancer chemotherapy consists in the lack of drug selectivity causing severe side effects. The targeted drug delivery appears to be a very promising strategy for controlling the biodistribution of the cytotoxic agent only on malignant tissues by linking it to tumor-targeting moiety. Here we exploit the natural characteristics of Shiga toxin B sub-unit (STxB) as targeting carrier on Gb3-positive cancer cells. Two cytotoxic conjugates STxB–doxorubicin (STxB–Doxo) and STxB–monomethyl auristatin F (STxB–MMAF) were synthesised using copper-free 'click' chemistry. Both conjugates were obtained in very high yield and demonstrated strong tumor inhibition activity in a nanomolar range on Gb3-positive cells.



## 1. Introduction

The development of new potent anticancer treatments has always presented a challenge, especially in cancer chemotherapy, where the lack of drug selectivity decreases the efficiency of the therapy leading to systematic toxicity and side effects. However targeted drug delivery was designed to circumvent this drawback.[1,2] The current strategies rely on the difference of the expressed surface receptors, metabolism profile and site location of the normal or cancerous cells. Indeed, the overexpression of cell surface molecules by tumor cells allows the use of specific ligands. To target only malignant tissues, the drug delivery systems are based on the coupling of cytotoxic drugs to tumor targeting carriers such as proteins, peptides, nucleic acid, carbohydrate and small molecules.[3,4] The most widely used targeting moieties are monoclonal antibodies (mAb). They are linked to the anticancer agent by lysine- or cysteine-based conjugation using different linker types: protease-, pH-, reductive cleavable linkers allowing the drug release inside the cell or in some case non-cleavable linker as thioether. In the last years two antibody–drug conjugates (ADCs) have been approved by FDA: brentuximab vedotin (Adcetris®) in 2011 and ado-trastuzumab emtansyne (Kadcyla®) in 2013.[5] They are considered as an essential improvement of chemotherapeutic agents for antitumoral treatment of Hodkins lymphoma and breast cancer.[5,6]

The mAb antibody has to fulfill a list of requirements such as being selective for tumor-associated antigens and humanized to minimize immunogenicity.[7–9] The antigen to which it is targeted should be highly expressed on the cell surface to enable efficient internalization and delivery of the cytotoxic payload. The anticancer agents typically used in ADCs are highly potent because the drug concentration is limited by antigen expression on the cellular membrane (typically less than $10^5$ per cell).[10] After cellular binding, ADCs are taken up by endocytosis and follow the lysosomal pathway where they undergo degradation, leading to the release of the cytotoxic drug. The linker between the antibody and the anticancer agent should be stable in circulation and efficiently cleaved inside tumor cells.[11–13] Another challenge for ADC preparation is to control the drug-to-antibody ratio (DAR) avoiding heterogeneous mixtures of conjugate species.

Natural ligands for cancer cell markers represent alternatives to antibodies. One of these is the B-subunit of Shiga toxin. This toxin is produced by *Shigella dysenteriae*, while enterohemorrhagic strains of *Escherichia coli* produce a family of Shiga-like toxins (or verotoxins). All these toxins are composed of toxic A-subunits and non-toxic receptor-binding B-subunits (STxB). STxB is a homopentameric protein composed of five identical B-fragments of 7.7 kDa. STxB binds to a glycosphingolipid, globotriaosylceramide ($Gb_3$), that is, overexpressed by human tumor cells.[14–19] STxB possesses 15 $Gb_3$ binding sites, and the apparent affinity for

* Corresponding author. Tel.: +33 156 246 664; fax: +33 156 246 6 31.
*E-mail address:* Frederic.Schmidt@curie.fr (F. Schmidt).

http://dx.doi.org/10.1016/j.bmc.2015.10.010
0968-0896/

cells is in order of $10^9$ $M^{-1}$. Once STxB recognizes $Gb_3$, the complex clusters on cell surface and induces membrane bending as a first step of its clathrin-independent uptake into cells.[14] The internalised protein then traffics through early and recycling endosomes and the *trans*-Golgi network (TGN) to the ER. This unconventional itinerary, termed the retrograde transport route, bypasses the late degrading environment of the late endocytic pathway.[14] STxB might therefore be used as a delivery tool to selectively transport cytotoxic compounds inside $Gb_3$-positive cells. For chemical cross-linking, a STxB variant is used to which a cysteine residue was added onto the C-terminus of each B-fragment, producing free thiol groups. In order to create STxB–drug conjugates, the conjugation reaction between STxB and prodrug must be accomplished in mild conditions in aqueous medium to preserve the integrity, the native conformation and functionality of the delivery tool. Unpublished studies performed in our team have demonstrated the loss of the STxB functionality when it was coupled to anticancer agent by copper catalyzed click reaction. Hence, bioorthogonal copper-free 'click' chemistry appears to be appropriate for the coupling of STxB to an anticancer agent.[20,21] The copper-free Huisgen [3+2] cycloaddition was reported as a very efficient reaction between cyclooctyne and azide where the ring strain of the alkyne drives the reaction forward without the use of catalyst.[24] Cyclooctyne and azide are inert to other functionalities present in biomolecules. Many biological applications have been reported where this coupling method did not interfere with protein structure and functions.[22,23] This chemistry thus proved to be adequate in satisfying many criteria such as biocompatibility, selectivity and especially high yield of coupling, which could avoid further protein purification problems.[25] Consequently, the copper-free Huisgen [3+2] cycloaddition appears to be a suitable choice for our carrier.

Here we explore the effectiveness of $Gb_3$-targeting delivery system using STxB conjugates prepared by versatile and modular copper-free click-based method. The targeting moiety is first functionalized with heterobifunctional linker **1** defined by maleimide functionalised monofluorocyclooctyne (MFCO) (Scheme 1). In this way the genetically modified STxB/Cys with 5 thiol functionalities is linked to the maleimide by thioether bond. In a second step, the click coupling between STxB–MFCO and azido-biotin **2** or the azido-prodrugs **3**, **4** are performed. The active principles of azido-prodrugs **3** and **4** are linked to STxB via their amine functionalities. Their scaffold was designed with disulfide bonds necessary to trigger, after reduction, the self-immolative mechanism and the drug release. The STxB–biotin conjugate is used for proof of concept demonstration. The two other STxB–drug conjugates aim to validate the efficiency of the targeting strategy, the drug releasing mechanism and optimize the anticancer treatment effect by introducing a highly potent anti-tumoral agent.

The anticancer agents chosen for the study are doxorubicin (Doxo) and monomethylauristatin F (MMAF) both containing free amine function in their respective structures. Doxo is a topoisomerase II inhibitor having DNA intercalating properties. The compound possesses high water solubility, but its use in the clinics is limited by detrimental side effects such as cardiotoxicity. MMAF is a derivative of the natural product dolostatin 10 with potent microtubulin inhibition activity. Its C-terminal domain is negatively charged at physiological pH, which makes MMAF little prone to cross the cell membrane spontaneously. Previous studies have shown the potentiated inhibition activity of its analog monomethyl auristatin E (MMAE) via antibody–drug conjugate (ADC), suggesting that impaired translocation capabilities of MMAF are the reason for its mild activity.[11] It has been demonstrated as well that the amine functions of Doxo and MMAF can be manipulated in order to create prodrugs for which the cytotoxic principle is released only once they target cells are reached.[11,26]

## 2. Results and discussion

### 2.1. Proof of concept: Synthesis of STxB–biotin conjugate

STxB–biotin conjugate was synthesized to test protein functionality after using copper-free cycloaddition on STxB. MFCO was chosen because of the balance between reactivity and synthesis accessibility of the molecule. The synthesis of bifunctional linker **1** started by preparation of MFCO **5** following a four step synthesis scheme described by Pigge from commercially available cyclooctanone.[27] The acid function of MFCO was coupled to the amine of a previously synthesised *N*-(2-aminoethyl)maleimide **6**. Compound **6** was obtained in two steps from Mitsunobu reaction between maleimide and Boc-ethanolamine followed by deprotection[28] (Scheme 2).

Several studies have reported side reactions of a thiol function on an alkyne.[29] To confirm the selectivity of MFCO toward the cycloaddition, we tested the reactivity of monofluorocyclooctyne **5** in the presence of cysteine methyl ester in organic medium. The reaction did not show any progress after 48 h at room temperature. Based on these results, compound **1** went through Michael addition with the free sulfhydryl residues of each STxB/Cys monomer. In parallel an azide-functionalised biotin **2** was obtained from peptide coupling between biotin and 1-amino-11-azido-3,6,9-trioxaundecane chosen for its hydrosolubility and commercial availability.[30] Then the intermediate STxB–MFCO **7** was coupled by copper free Huisgen [3+2] cycloaddition to linker **2** to afford conjugate **8** (Scheme 2). The yield and purity of each step were monitored by LC–MS analysis. The yields of the two steps were respectively of 85% and 95% for a 1:1 stoichiometry between biotin and STxB monomer.

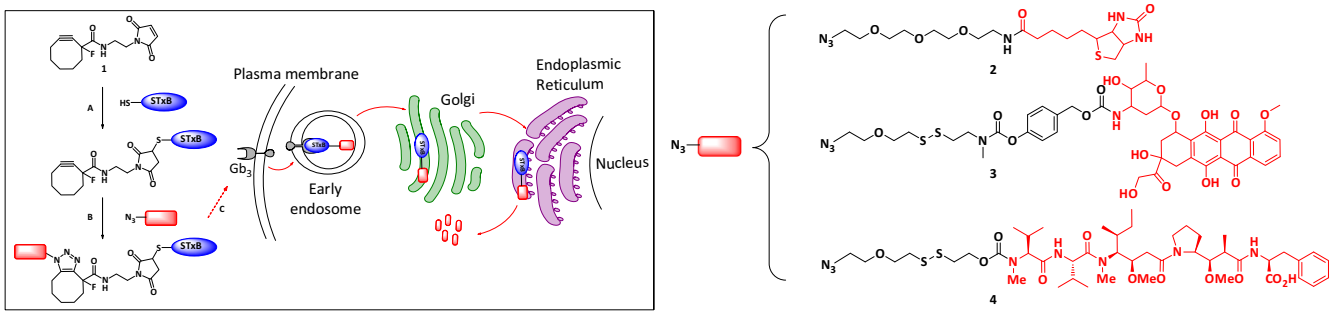


**Scheme 1.** Click synthesis and retrograde delivery strategy. (A) Bifunctional linker **1** coupling with STxB/Cys, (B) Cu-free click ligation with azido-probiotin **2** or azido-prodrug **3** and **4**, (C) tumor-specific drug delivery induced by STxB on positive Gb3 cells.

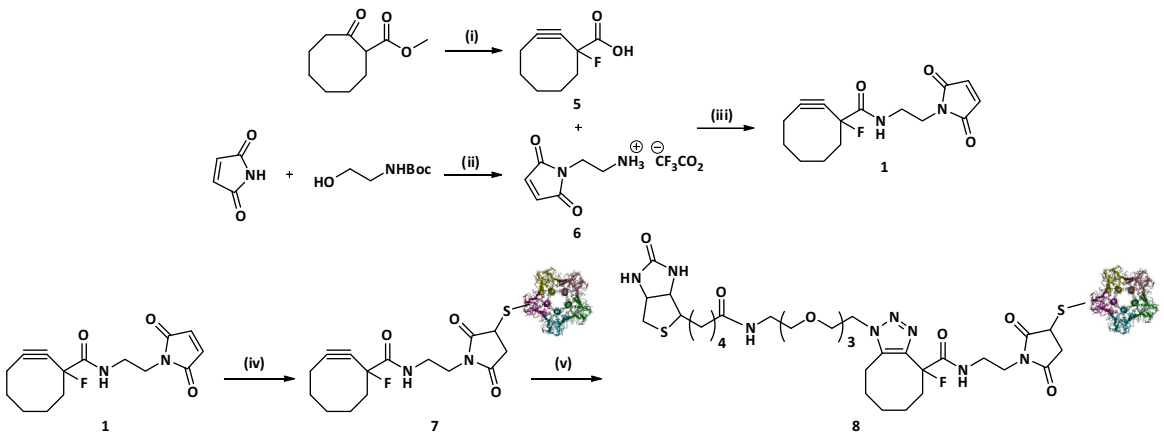

**Scheme 2.** Synthesis of bifunctional linker **1** and STxB–biotin conjugate **8**. Reagents and conditions: (i) (a) Selectfluor,$CH_3CN$, reflux, (93%); (b) KHMDS, $Tf_2NPh$, THF, −80 °C, (60%); (c) LiOH, THF, (92%); (ii) (a) DEAD, $PPh_3$, THF, −78 °C, (80%); (b) TFA, $CH_2Cl_2$, (87%); (iii) (a) PFP–TFA, DIPEA, $CH_2Cl_2$; (b) DIPEA, DMF, (78%); (iv) STxB/Cys, PBS buffer, 21 °C, 18 h, (85%); (v) **2**, PBS buffer, 21 °C, 18 h, (95%).

## 2.2. Biological assessment of STxB–biotin conjugate

STxB–biotin conjugate was tested for its ability to be internalized into $Gb_3$-positive cells and to follow the retrograde trafficking route. To validate the concept, the unmodified STxB/Cys and conjugate **8** were followed by immunofluorescence analysis on HeLa cells after 45 min incubation at 37 °C. Co-localization of conjugate **8** with the Golgi marker giantin, was similar to this observed for the non-modified STxB/Cys (Scheme 3).

The cellular uptake characteristics of STxB–biotin were obviously preserved and the carrier was functional. We concluded that the copper free cycloaddition was compatible with STxB targeting strategy and it can be used for the design of STxB–prodrug conjugates.

## 2.3. Design and synthesis of STxB–Doxo conjugate

To exploit some of the previous mentioned properties of STxB and release a drug inside $Gb_3$ positive tumors cells after carrier-mediated targeting, we designed and synthesized conjugate **16** (Scheme 6). We choose to rely on disulfide bonds able to be reductively cleaved and to trigger drug release. Doxorubicin (Doxo) appeared to be a good candidate for testing the targeting strategy showing good hydrosolubility and cytotoxic activity toward HT 29 colon carcinoma cell lines. However the drug itself does not possess a thiol so we built a spacer able to liberate the amino-bearing anticancer agent after cleavage of the disulfide. The scaffold of the linker is defined by an azide function that is linked by a small PEG to the disulfide bond, followed by a biocleavable spacer enabling the drug delivery. Previous work of the laboratory[31] demonstrated that a 2-amino-ethanethiol can release a phenol through disulfide reduction. If the phenol is a 4-hydroxybenzyl alcohol, it can be used to release the drug amino group. Based on the literature, we suggest the following mechanism of drug release[32] (Scheme 4).

Firstly we prepared linker **3** starting by deacetylation dimerization of compound **9** previously synthesized in two steps from 2-chlorethoxyethanol, affording derivative **10**[33] (Scheme 5). The next step was a dismutation between **10** and **11**[31] prepared from commercially available methylaminoethanol. The corresponding *tert*-butoxycarbonyl derivative **12** went through a classical deprotection in acidic conditions. The obtained salt **13** was condensed with p-nitrophenyl carbonate derivative **22** previously obtained in two steps from commercial 4- hydroxybenzyl alcohol.[32] The instability of the TBDMS ether in mild acid conditions was used to deprotect the primary alcohol of **14** so it could be reactivated by 4-nitrophenyl chloroformate to afford final activated linker **15**. Doxorubicin was then coupled to spacer **15** in basic conditions giving derivative **3** (Scheme 6). Compound **3** was finally coupled to STxB–MFCO **7** in PBS buffer and MALDI-TOF spectrometry validated the formation of the conjugate.

The mass spectrum displayed a major peak for the final conjugate **16** and a minor peak at 8646 Da. This minor peak could be attributed to a byproduct of the conjugate without the aromatic planar chromophore of doxorubicin, probably due to the photosensitivity of the drug. The conjugate **16** was produced with the maximum substitution (5 molecules of doxorubicin per pentamer of STxB). The yield for the final click reaction was 89 % as determined by LC–MS analysis.

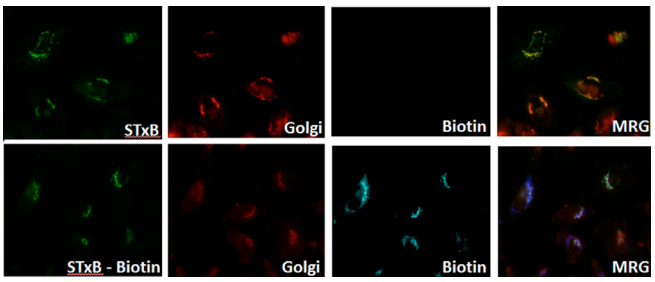


**Scheme 3.** Retrograde trafficking of STxB and STxB–biotin conjugate. STxB or STxB–biotin were bound to HeLa cells at 4 °C, followed by incubation for 45 min at 37 °C. Cells were fixed and labeled for the indicated markers. Top: STxB; bottom: STxB–biotin conjugate **8**. STxB: green; giantin: red; Biotin: blue; MRG: merge.

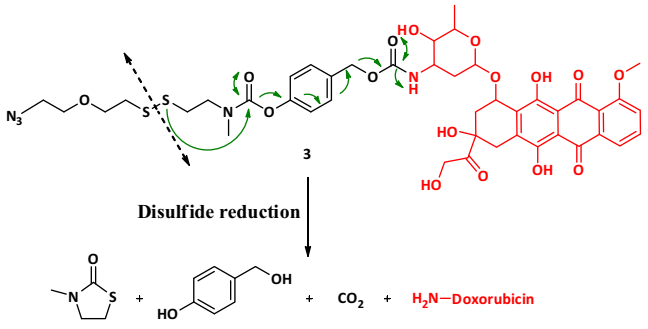


**Scheme 4.** Release mechanism of doxorubicin by reduction of disulfide bond followed by 1,6-elimination.

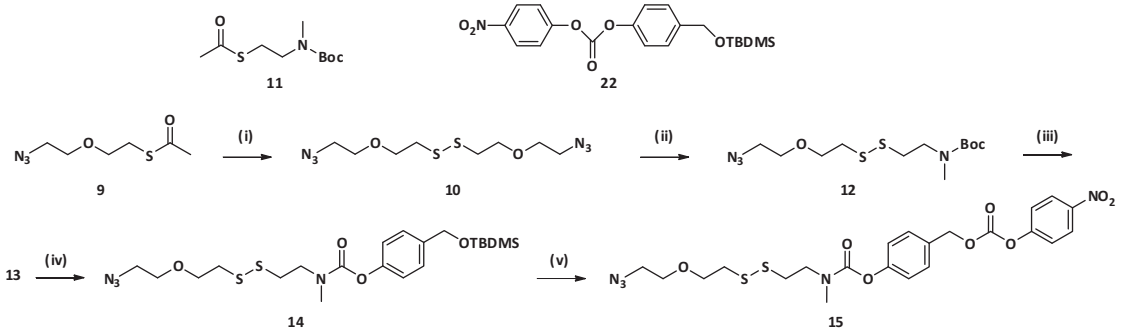

**Scheme 5.** Azido-linker **15** synthesis. Reagents and conditions: (i) MeONa (0.5 M), MeOH, rt, overnight under air (70%); (ii) **11,** MeONa, MeOH, rt, (72%); (iii) (a) TFA, DCM, rt, (quant.); (iv) **22**, $Et_3N$, DMF, rt, (87%); (v) (a) HCl (12 N) at 10% in EtOH, rt, (95%); (b) $pNO_2PhOCOCl$, $Et_3N$, DCM, rt, (66%).

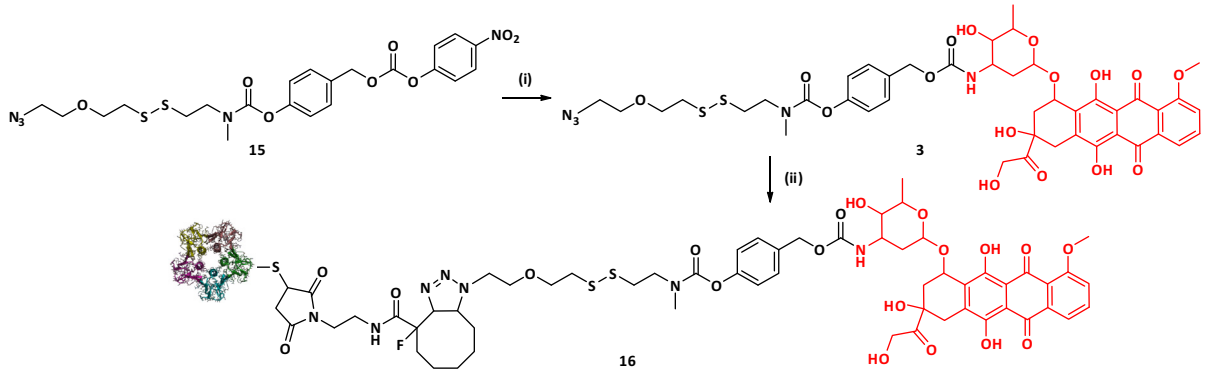

**Scheme 6.** Synthesis of STxB–doxorubicin conjugate **16**. Reagents and conditions: (i) doxorubicin, $Et_3N$, DMF, (50%); (ii) compound **7**, PBS buffer, 21 °C, 18 h, (89%).

## 2.4. Cytotoxicity of STxB–Doxo conjugate

The cytotoxic activity of STxB–Doxo conjugate was tested using a MTT colorimetric assay on $Gb_3$ positive colorectal carcinoma cells HT29. To generate a Gb3-negative control condition, HT29 cells were treated with the glycosylceramide synthetase inhibitor 1-phenyl-2-palmitoylamino-3-morpholino-1-propanol (PPMP) to inhibit glycosphingolipid synthesis. Cytotoxicity assay revealed the specificity of the STxB targeting strategy, showing cytotoxic activity of STxB–Doxo conjugate **16** only on $Gb_3$ positive HT29 cells. As expected the toxicity of free Doxo and the linker **3** was Gb3 independent (Scheme 7). The $IC_{50}$ values of free doxorubicin and conjugate **16** were in the same range of 84.8 and 22.5 nM, respectively, (Table 1). This result demonstrates that the self-immolative drug release mechanism is functional.

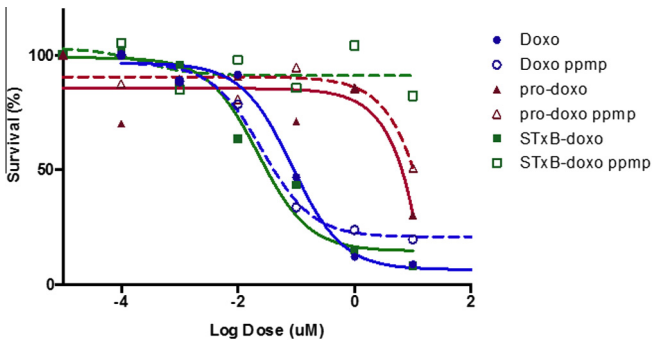


**Scheme 7.** Comparison of cytotoxicity of the conjugate STxB–Doxo **16** on Gb3+ and Gb3− (PPMP treated) HT29 cells.

**Table 1**
$IC_{50}$ values of STxB–Doxo conjugate **16** on Gb3+ versus Gb3− (PPMP treated) HT29 cells in comparison to untargeted doxorubicin and pro-Doxo **3**

| Cytotoxic activity on HT **29** | $IC_{50}$ (nM) Gb3+ | $IC_{50}$ (nM) Gb3− |
|---|---|---|
| Doxorubicin | 84.8 | 25.9 |
| Prodrug **3** | 6000 | 10,000 |
| STxB–Doxo **16** | 22.5 | – |

The experiment confirmed the functionality and the efficiency of the STxB drug delivery strategy with an increased activity of the anticancer agent on tumor cells. The intracellular uptake of conjugate was tested in vitro and confirmed the protein integrity of **16**.

## 2.5. Design and synthesis of STxB–MMAF conjugate

To optimize the established targeting strategy we replaced doxorubicin with a more potent anticancer agent, monomethyl auristatin F (MMAF), using the same self-immolative spacer **15** (Scheme 8). We proceed with coupling between derivative **15** and MMAF in basic conditions affording compound **23**. The copper-free reaction between STxB–MFCO **7** and **23** gave less than 10% yield. It seemed likely that a solubility problem could explain the low yields. Assays were therefore performed at different temperatures, buffer conditions, linker arms, and STxB–MFCO concentrations, but reactivity remained similarly low. A second hypothesis was that steric hindrance at the azide group position prevented the cycloaddition with MFCO, due to a conformational restriction resulting for example from π–π stacking between the two aromatic rings in the structure of compound **23** (Scheme 8).

In order to test this hypothesis, we replaced the phenyl carbamate by a simple carbamate linked to the amine extremity of MMAF.[34] The synthesis of the linker **4** started with hydrolysis of

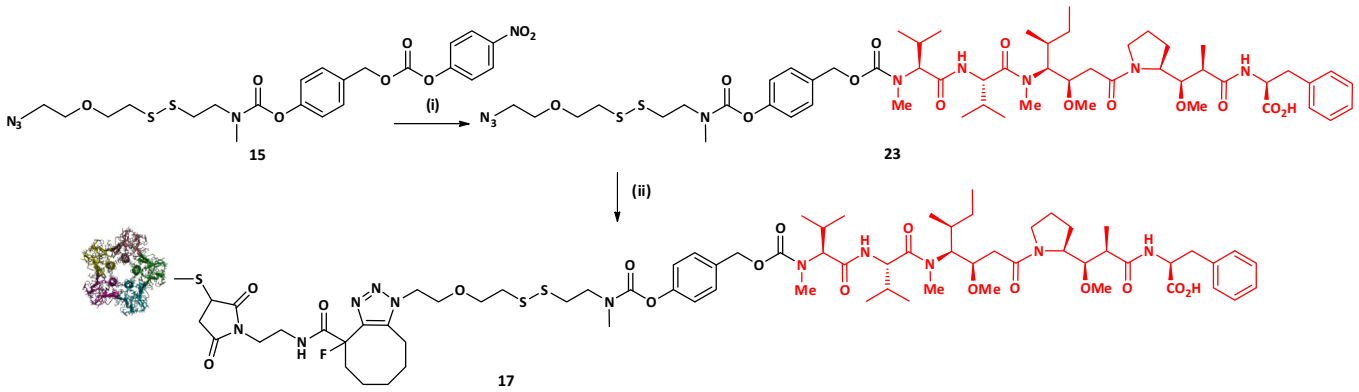

**Scheme 8.** Synthesis of STxB–MMAF conjugate **17**. Reagents and conditions: (i) MMAF, $Et_3N$, DMF, rt, overnight, (60%); (ii) compound **7**, PBS buffer, 21 °C, 18 h, (10%).

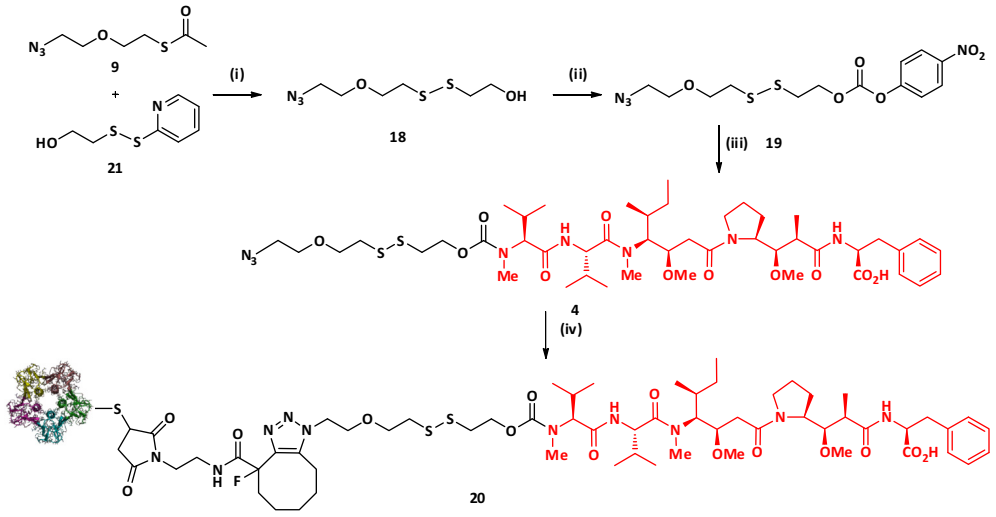

**Scheme 9.** Synthesis of STxB–MMAF conjugate **20**. Reagents and conditions: (i) MeONa (0.5 M), MeOH, rt, (79%); (ii) $pNO_2PhOCOCl$, $Et_3N$, DCM, rt, (75%); (iii) MMAF, $Et_3N$, DMF, rt (71%); (iv) compound **7**, PBS buffer, 21 °C, 18 h, (94%).

the thioacetate function of **9** generating in situ a free thiol group that was trapped by nucleophilic attack with disulfide compound **21**[35] (Scheme 9). The resulting disulfide **18** was activated with 4-nitrophenyl chloroformate to afford the activated linker **19**. The MMAF condensation with compound **19** then afforded the azide–pro MMAF derivative **4**. The synthesis was pursued with incubation of linker **4** and STxB–MFCO conjugate **7** in PBS buffer yielding the desired STxB–MMAF conjugate **20**. LC–MS analysis confirmed 94% yield for the final step of copper free Huisgen cycloaddition [3+2]. This result is consistent with our hypothesis of steric hindrance lowering the reactivity of the azide group toward the cycloaddition with MFCO.

## 2.6. Cytotoxicity of STxB–MMAF conjugate

Conjugate **20** displayed potent cytotoxic activity on $Gb_3$-expressing HT29 cells with an $IC_{50}$ value of 8.4 nmol (Table 2).

**Table 2**
$IC_{50}$ values of STxB–MMAF conjugate **20**on Gb3+ versus Gb3− (PPMP treated) HT29 cells in comparison to untargeted MMAF

| Cytotoxic activity on HT **29** | $IC_{50}$ (nM) Gb3+ | $IC_{50}$ (nM) Gb3− |
|---|---|---|
| MMAF | 43.5 | 37.5 |
| STxB–MMAF **20** | 8.4 | 1500 |

In comparison, the untargeted MMAF had an $IC_{50}$ value of 43 nM. Conjugate **20** was around 200 folds less toxic on PPMP-treated cells confirming that STxB conjugation promotes a $Gb_3$-specific cell internalization of MMAF (Scheme 10). The data also demonstrated an improved efficiency and highlighted the selectivity of the STxB-based MMAF delivery strategy, which enhanced the cytotoxic effect of the anticancer agent on $Gb_3$-positive tumor cells. The STxB–MMAF conjugate was evaluated in vitro for its intracellular trafficking characteristics. Accumulation in the Golgi apparatus

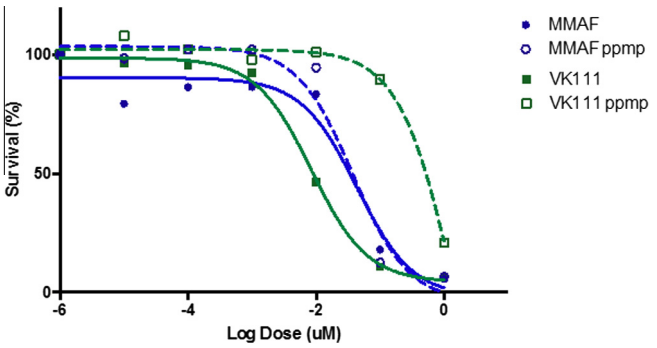


**Scheme 10.** Cytotoxicity of the STxB–MMAF conjugate on Gb3+ versus Gb3− (PPMP treated) HT29 cells.

**Table 3**
$IC_{50}$ values of STxB–MMAF conjugate **20** on Gb3+ versus Gb3− (PPMP treated) HT29 cells with or without pre-incubation in pure serum (SVF)

| Cytotoxic activity on HT **29** | $IC_{50}$ (nM) no pre-incubation | | $IC_{50}$ (nM) pre-incubation | |
|---|---|---|---|---|
| | Gb3+ | Gb3− | Gb3+ | Gb3− |
| MMAF | | | 64 | 60 |
| STxB–MMAF **20** | 6.6 | 580 | 5.6 | 380 |

was as efficient for conjugate **20** as for STxB/Cys, confirming that the functional integrity of the protein was preserved despite the presence of the MMAF.

In order to test the stability of the conjugate in the light of future animal experiments, the cytotoxic activity of conjugate **20** was measured with and without 24 h pre-incubation at 37 °C in pure SVF serum. We observed similar activity, makes it likely that the conjugate could be biodistributed in an intact manner before the liberation of the active principle in cancerous target cells (Table 3).

## 3. Conclusion

The work presented herein proposes a novel targeting approach for amine-containing anticancer agents, using the non-toxic B-subunit of Shiga toxin (STxB) as a delivery tool. We used an efficient synthetic strategy where protein integrity was preserved by exploiting copper free Huisgen [3+2] cycloaddition. The catalyst-free bioorthogonal reaction allowed to obtain very high yields of coupling between the linkers and STxB. The conjugates STxB–Doxo and STxB–MMAF demonstrated potent cytotoxic activity and proved the versatility of the drug releasing mechanism of disulfide bonds linked to carbamate systems. Our data also highlight that the nature of carbamate and the structure of the anticancer agent can influence the coupling yields between STxB and drug linker, for instance by an imposed conformation. Finally, STxB–Doxo and STxB–MMAF showed high selectivity and potency on Gb3-positive HT29 cells, with $IC_{50}$ values in nanomolar range. These conjugates are now entering in vivo evaluation in mice.

## 4. Experimental part

### 4.1. General chemistry methods

Reactions were performed under inert atmosphere (nitrogen) unless otherwise stated. THF was distilled from sodium and benzophenone, $CH_2Cl_2$ was distilled from $P_2O_5$. DMF and methanol were stored over molecular sieves. Commercial products were used without further purification. TLC (0.25 mm silica gel 60-F plates) was used to follow the reaction. Visualization was accomplished with UV light (254 nm), ammonium molybdate or ninhydrin. Flash chromatographies were carried out on 320–400 mesh size silica gel. $^1$H NMR and $^{13}$C NMR spectra were recorded on a BRUCKER ACP 300 at respectively 300 MHz and 75 MHz. Chemical shifts are reported in ppm relative to the residual solvent peak as the internal reference, coupling constants *J* are given in Hertz. Spin multiplicities are given with the following abbreviations: s = singlet, d = doublet, dd = doublet of doublet, t = triplet, q = quadruplet, m = multiplet. Positive and negative electrospray ionization spectra were performed on a WATERS ZQ 2000. High resolution mass spectra were obtained at the Laboratoire de Spectrométrie de Masse of Chimie Paris Tech. Mass spectroscopy for compounds containing a protein moiety was conducted on a Voyager-DE PRO MALDI-TOF mass spectrometer (Applied Biosystems, Framingham, USA) operated in the delayed extraction and linear mode. The matrix was composed by a solution of sinapinic acid in acetonitrile/TFA. Samples were mixed with the matrix at a ratio of 1:1. The mixture was spotted onto a MALDI-TOF plate and allowed to dry.

### 4.2. Synthesis and characterization of described compounds

#### 4.2.1. 1-Fluoro-cyclooct-2-ynecarboxylic acid [2-(2,5-dioxo-2,5-dihydro-pyrrol-1-yl)-ethyl]-amide (1)

Pentafluorophenyl trifluoroacetate (0.70 g, 2.52 mmol, 433 μL) was added to a solution of 1-fluorocyclooct-2-ynecarboxylic acid **5** (0.36 g, 2.12 mmol) and *N*,*N*-diisopropylethylamine (0.32 g, 2.52 mmol, 438 μL) in dry DCM (21 mL) brought to 0 °C. The mixture was stirred at room temperature for 3 h and filtered over silica. The activated acid (0.85 g, 2.55 mmol), *N*-(2-aminoethyl)-maleimide **6** (0.34 g, 3.19 mmol) and *N*,*N*-diisopropylethylamine (0.39 g, 3.06 mmol, 533 μL) were agitated in dry DMF (41 mL) for 16 h at room temperature. Distilled water (20 mL) was added. The organic phase was extracted with DCM (3 × 30 mL), washed with brine (80 mL) and dried over $MgSO_4$. After filtration the mixture was concentrated in vacuum. Purification over silica gel (EtOAc/hexane, 20:80–30:70) afforded **1** (0.38 g, 61%). $R_f$ = 0.45 (EtOAc/hexane, 1:1). $^1$H NMR ($CDCl_3$, 300 MHz): $\delta$ 6.72 (s, 2H), 3.71 (m, 2H), 3.54 (m, 2H), 2.29 (m, 4H), 1.93 (m, 4H), 1.62 (m, 1H), 1.44 (m, 1H); $^{13}$C NMR ($CDCl_3$, 75 MHz) $\delta$ (ppm): 171.4, 169.2 (d), 134.7, 109.7 (d), 96.0, 93.5, 87.2 (d), 46.3 (d), 39.2, 37.5, 34.2, 29.3, 26.0, 21.1; MS (ES+ for $C_{15}H_{17}FN_2O_3$): *m*/*z* = 293 [M+H$^+$], 315 [M+Na$^+$], calcd 292.

#### 4.2.2. 1.2-Bis(2-(2-azidoethoxy)ethyl disulfane (10)

To a solution of *S*-(2-(2-azidoethoxy)ethyl)ethanethiolate **9** (1.89 g, 10 mmol) in dry MeOH (75 mL) purged in argon for 30 min was added NaOMe (2.17 mL, 25% w/v, 10 mmol). The reaction mixture was stirred under air overnight at room temperature. DOWEX was added until pH 6. After concentration in vacuum, the crude product was purified on a silica gel column (EtOAc/cyclohexane, 10:90). Disulfide **10** was obtained as yellow oil (2.05 g, 70%). $R_f$ = 0.4 (EtOAc/cyclohexane, 10:90). $^1$H NMR ($CDCl_3$, 300 MHz): $\delta$ 3.76 (t, *J* = 6.5 Hz, 2H), 3.66 (t, *J* = 4.9 Hz, 2H), 3.40 (t, *J* = 6.5 Hz, 2H), 2.90 (t, *J* = 4.9 Hz, 2H). $^{13}$C NMR ($CDCl_3$, 75 MHz): $\delta$ 69.8, 69.5, 50.7, 38.4. MS (ESI for $C_8H_{16}N_6O_2S_2$): *m*/*z* 293 [M+H$^+$], calcd 292.

#### 4.2.3. *tert*-Butyl(2-((2-(2-azidoethoxy)ethyl)disulfanyl)ethyl)(methyl)carbamate (12)

NaOMe (0.68 mL of 0.5 M in MeOH, 10 mmol) was added dropwise to a stirred solution of *S*-2-(*tert*-butoxycarbonyl(methyl)amino)ethyl ethanethioate **11** (1.2 g, 5.13 mmol) and **10** (1.5 g, 5.13 mmol) in anhydrous MeOH (28 mL). The reaction was stirred overnight under an argon atmosphere. The residue was purified by flash chromatography over silica (EtOAc/Hexane, 1:1) to afford **12** as a clear, pale yellow liquid (1.24 g, 72%). $R_f$ = 0.4 (EtOAc/cyclohexane, 1:1). $^1$H NMR ($CDCl_3$, 300 MHz): $\delta$ 3.76 (t, *J* = 6.5 Hz, 2H), 3.66 (t, *J* = 4.8 Hz, 2H), 3.47 (t, *J* = 6.6 Hz, 2H), 3.39 (t, *J* = 6.6 Hz, 2H), 2.90 (t, *J* = 6.5 Hz, 2H), 2.89 (s, 3H), 2.82 (m, 2H), 1.44 (s, 9H). $^{13}$C NMR ($CDCl_3$, 75 MHz): $\delta$ 155.5, 80.0, 70.1, 69.9, 69.8, 51.0, 48.75, 43.8, 38.7, 38.6 36.8, 36.6, 35.2, 30.5, 28.8, 27.2. MS (ESI for $C_{12}H_{24}N_4O_3S_2$): *m*/*z* 337 [M+H$^+$], calcd 336.

#### 4.2.4. 2-((2-(2-Azidoethoxy)ethyl)disulfanyl)-*N*-methylethan aminium 2,2,2 trifluoroacetate (13)

TFA (5 mL) was added to a solution of **12** (1.2 g, 5.06 mmol) dry DCM (10 mL). The yellow solution was stirred at room temperature for 1 h. The mixture was evaporated under vacuum. The resulting product was used without further purification. $R_f$ = 0.0 (acetone/DCM, 10:90). $^1$H NMR ($CDCl_3$, 300 MHz): $\delta$ 3.69 (t, *J* = 6.6 Hz, 2H),

3.57 (t, $J$ = 4.8 Hz, 2H), 3.33 (t, $J$ = 6.5 Hz, 2H), 3.26 (t, $J$ = 6.5 Hz, 2H), 2.87 (t, $J$ = 6.6 Hz, 2H), 2.82 (m, 2H), 2.77 (s, 3H). $^{13}$C NMR ($CDCl_3$, 75 MHz): $\delta$ 69.9, 68.0, 50.0, 47.2, 37.1, 33.0, 32.7, 32.1. MS (ESI for $C_7H_{16}N_4OS_2$): $m/z$ 237 [M+H$^+$], calcd 236.

#### 4.2.5. 4-(((*tert*-Butyldimethylsilyl)oxy)methyl)phenyl(2-((2-(2-azidoethoxy)ethyl)disulfanyl)ethyl)(methyl)carbamate (14)

Triethylamine (1.3 ml, 9.28 mmol) was added dropwise to a solution of **13** (1.1 mg, 4.64 mmol) in DMF (10 mL) followed by addition of 4-((*tert*-butyl dimethyl silyl)oxy)methyl)phenyl(4-nitrophenyl)carbonate **22** (936 mg, 2.32 mmol). The mixture was agitated overnight at room temperature. After the evaporation, the crude product was purified on silica gel (acetone/DCM, 0:100–8:92) to afford colorless oil **14** (1.00 g, 87%). $R_f$ = 0.3 (acetone/DCM, 5:95). $^1$H NMR ($CDCl_3$, 300 MHz): $\delta$ 7.32 (d, $J$ = 15.9 Hz, 2H), 7.08 (d, $J$ = 15.9 Hz, 2H), 4.71 (s, 2H), 3.75 (t, $J$ = 6.6 Hz, 2H), 3.65 (m, 2H), 3.63 (m, 3H), 3.37 (m, 2H), 3.15–3.05 (s, 3H), 2.95 (m, 2H), 2.91 (m, 2H), 0.93 (s, 9H), 0.08 (s, 6H). $^{13}$C NMR ($CDCl_3$, 75 MHz): $\delta$ 150.7, 127.9, 126.1, 121.9, 115.6, 69.8, 64.9, 50.6, 38.0, 33.1, 29.16, 0.05. MS (ESI for $C_{21}H_{36}N_4O_4S_2$-Si): $m/z$ 501 [M+H$^+$], calcd 500.

#### 4.2.6. 4-((((4-Nitrophenoxy)carbonyl)oxy)methyl)phenyl(2-((2-(2-azidoethoxy)ethyl)disulfanyl)ethyl)(methyl)carbamate (15)

HCl 1% (64 μL) was added to a solution of **14** (1 g, 2.02 mmol) in EtOH (6.3 mL). The mixture was stirred for 1 h at room temperature. After evaporation the residue (296 mg, 0.77 mmol) were diluted in anhydrous DCM (15 mL). To the solution was added dropwise triethylamine (310 μL, 2.3 mmol) and 4-nitrophenylchloroformate (309 mg, 1.53 mmol). The mixture was stirred for 2 h at room temperature and purified over silica (EtOAc/cyclohexane, 30:70) to afford compound **15** (280 mg, 66%). $R_f$ = 0.6 (EtOAc/cyclohexane, 10:90). $^1$H NMR ($CDCl_3$, 300 MHz): $\delta$ 8.28 (d, $J$ = 9.3 Hz, 2H), 7.46 (d, $J$ = 8.4 Hz, 2H), 7.39 (d, $J$ = 9.3 Hz, 2H), 7.18 (d, $J$ = 8.4 Hz), 5.27 (s, 2H), 3.75 (t, $J$ = 6.9 Hz, 2H), 3.65 (q, $J$ = 4.2 Hz, 2H), 3.640 (t, $J$ = 5.1 Hz, 2H), 3.38 (q, $J$ = 4.2, 2H), 3.16–3.05 (s, 3H), 2.94 (m, 2H), 2.91 (m, 2H). $^{13}$C NMR ($CDCl_3$, 75 MHz): $\delta$ 155.4, 154.2, 152.1, 151.8, 145.5, 131.0, 130, 125.3, 122.1, 70.3, 69.7, 69.4, 50.3, 48.9, 48.4, 38.1, 36.0. MS (ESI for $C_{22}H_{25}N_5O_8S_2$): $m/z$ 551 [M+H$^+$], calcd 552.

#### 4.2.7. 4-((Carbamoyloxy)methyl)phenyl(2-((2-(2-azidoethoxy)ethyl)disulfanyl)ethyl)(methyl)carbamate doxorubicin (3)

To a mixture of **15** (20 mg, 0.036 mmol) and doxorubicin (12 mg, 0.022 mmol) in DMF (1 mL) was added pyridine (3 μL, 0.037 mmol) and triethylamine (3 μL, 0.022 mmol). The solution was stirred overnight at room temperature. After evaporation the residue was purified over silica gel (MeOH/DCM, 0:100–3:97) to give product **3** (17 mg 81%). $R_f$ = 0.31 (acetone/cyclohexane, 1:1). MS (MALDI-TOF$^+$ for $C_{43}H_{49}N_5O_{16}S_2$): $m/z$ 978 [M+Na$^+$], 994 [M+K$^+$], calcd 956.

#### 4.2.8. 4-((Carbamoyloxy)methyl)phenyl(2-((2-(2-azidoethoxy)ethyl)disulfanyl)ethyl)(methyl)monomethylauristatin F (23)

Triethylamine (6.5 μL, 0.048 mmol) was added to **15** (8.8 mg, 0.016 mmol), MMAF (12 mg, 0.016 mmol) in anhydrous DMF (800 μL). The solution was stirred at room temperature overnight. After evaporation the crude product was purified over silica gel (MeOH/DCM, 0:100–8:92) to obtain compound **23** (11 mg, 60%). $R_f$ = 0.23(MeOH/DCM, 10:90). MS (MALDI-TOF$^+$ for $C_{55}H_{85}N_9O_{13}S_2$): $m/z$ 1166 [M+Na$^+$], calcd 1133.

#### 4.2.9. 2-((2-(2-Azidoethoxy)ethyl)disulfanyl)ethanol (18)

A solution of *S*-2-(2-azidoethoxy)ethyl ethanethioate **9** (648 mg, 3.42 mmol) and sodium methoxide (0.5 M, 3 mL) in anhydrous MeOH (32 mL) was stirred at room temperature under argon atmosphere for 1 h. The solution was quenched with AcOH and evaporated. Then 2-(pyridin-2-yldisulfanyl)ethanol **21** (580 mg, 3.1 mmol) was added to the intermediate diluted in MeOH (35 mL) and the mixture was stirred overnight at room temperature. After evaporation, the crude product was purified by column chromatography over silica (AcOEt/cyclohexane, 10:90–20:80) to afford product **18** (601 mg, 79%). $R_f$ = 0.51 (Acetone/cyclohexane, 1:1). $^1$H NMR ($CDCl_3$, 300 MHz): $\delta$ 3.89 (t, $J$ = 5.7 Hz, 2H), 3.76 (t, $J$ = 6.6 Hz, 2H), 3.65 (t, $J$ = 4.8 Hz, 2H), 3.39 (t, $J$ = 5.1 Hz, 2H) 2.88 (m, 4H). $^{13}$C NMR ($CDCl_3$, 75 MHz): $\delta$ 69.7, 69.5, 60.2, 50.6, 41.3, 38.2. MS (ESI for $C_6H_{13}N_3O_2S_2$): $m/z$ 224 [M+H$^+$], calcd 223.

#### 4.2.10. 2-((2-(2-Azidoethoxy)ethyl)disulfanyl)ethyl(4-nitrophenyl)carbonate (19)

Pyridine (421 μL, 5.212 mmol) and 4-nitrophenylchloroformate (787 mg, 3.9 mmol) were added to solution of **18** (582 mg, 2.61 mmol) in DCM (10 mL). After overnight stirring at room temperature, the residues were purified over silica gel (DCM, 100%) to give product **19** (765 mg, 75%). $R_f$ = 0.32 (acetone/cyclohexane, 20:80). $^1$H NMR ($CDCl_3$, 300 MHz): $\delta$ 8.29 (d, $J$ = 8.9 Hz, 2H), 7.40 (d, $J$ = 9.3 Hz, 2H), 4.55 (t, $J$ = 6.6 Hz, 2H), 3.76 (t, $J$ = 6.6 Hz, 2H), 3.66 (d, $J$ = 4.8 Hz, 2H), 3.39 (d, $J$ = 5.1 Hz, 2H) 3.03(t, $J$ = 6.6 Hz, 2H), 2.94 (t, $J$ = 6.6 Hz, 2H). $^{13}$C NMR ($CDCl_3$, 75 MHz): $\delta$ 156.4, 153.5, 146.8, 125.7, 122.1, 70.9, 69.7, 67.3, 51.0, 38.9, 36.9. MS (ESI for $C_{13}H_{16}N_4O_6S_2$): $m/z$ 389 [M+H$^+$], calcd 388.

#### 4.2.11. 2-((2-(2-Azidoethoxy)ethyl)disulfanyl)ethyl carbonyle mono-methylausristatin F (4)

Compound **19** (18 mg, 0.046 mmol), MMAF (17 mg, 0.023 mmol), triethylamine (6.8 μL, 0.050 mmol) and HOBt (4 mg, 0.029 mmol) were stirred in THF (600 μL) overnight at room temperature. After evaporation, the crude product was purified by chromatography (MeOH/DCM, 0:100–6:94) to afford **4** (16 mg, 71%). $R_f$ = 0.26 (MeOH/DCM, 5:95). MS (MALDI-TOF$^+$ for $C_{46}H_{76}N_8O_{11}S_2$): $m/z$ 1003 [M+Na$^+$], 1019 [M+K$^+$], calcd 980.

### 4.3. Coupling with STxB

The coupling reactions were performed with genetically engineered STxB/Cys containing five C-terminal cysteine residues purified according to established procedures.[36] MALDI-TOF mass spectrometry was used to follow the formation of STxB-based conjugates with error in the range of ±5 Da. LC–MS analysis was used to determine the coupling yield. The cyclooctyne and prodrug compounds were dissolved in DMSO (10% DMSO final concentration in the reaction volume), and STxB/Cys diluted in a PBS buffer to a final concentration of 1 mg/mL. To determine the optimal reaction conditions STxB was incubated with tree different molar excess (1, 3 and 9) of cyclooctyne or prodrug per B-fragment monomer (note that STxB is a homopentamer of 5 B-fragments). Coupling reactions were carried out for 18 h at 21 °C with stirring, and the conjugates were dialyzed (10 kDa cut-off) for 3–24 h at room temperature or 4 °C, against water for MALDI analysis, or PBS for in vitro cytotoxicity testing.

STxB–MFCO, **7**: $m/z$ = 8085 (calcd), 8085 (found); STxB: $m/z$ = 7793 (calcd), 7792 (found).

STxB–biotin, **8**: $m/z$ = 8529 (calcd), 8531 (found); STxB: $m/z$ = 7793 (calcd), 7794 (found).

STxB–Doxo, **16**: $m/z$ = 9040 (calcd), 9042 (found); STxB: $m/z$ = 7793 (calcd), 7793 (found).

STxB–MMAF, **17**: $m/z$ = 9229 (calcd), 9334 (found); STxB: $m/z$ = 7793 (calcd), 7796 (found).

STxB–MMAF, **20**: $m/z$ = 9065 (calcd), 9069 (found); STxB: $m/z$ = 7793 (calcd), 7795 (found).

### 4.4. Intracellular retrograde trafficking evaluation by immunofluorescence

STxB conjugates were tested on HeLa cell at a final concentration of 50 nM (STxB pentamer). Cells were incubated for 30 min at 4 °C, washed, incubated for 45 min at 37 °C, fixed with 4% para-formaldehyde, washed again with 50 mM $NH_4Cl$ solution, and permeabilized with saponin (PBS/BSA/Saponin 1×). Immunodetection was conducted using a primary mouse-monoclonal anti-STxB antibody (13C4), and a home-made rabbit polyclonal antibody against the Golgi marker giantin, followed by detection using appropriate fluorescently labeled secondary antibody, or streptavidin in the case of biotin.

### 4.5. Inhibition of Gb3 synthase

Cells were incubated for 6 days with 5 mM of the glycosylceramide synthase inhibitor 1-phenyl-2-palmitoylamino-3-morpholino-1-propanol (PPMP). Gb3 expression was determined by FACS analysis after incubation with STxB-AlexaFluor488. PPMP treatment was scored successful when remaining fluorescent cell population was below 2% of that observed on non-PPMP treated control cells.

### 4.6. Cytotoxic activity evaluation

5000 HT 29 cells were seeded in 96-well dishes in DMEM medium 24 h before contact. STxB conjugates or uncoupled cytotoxic compounds were then incubated for 6 h at 37 °C with these cells. After extensive washes, cells were incubated for 5 additional days. A colorimetric assay (MTT) based on mitochondrial metabolism was carried out to determine the percentage of living cells. $IC_{50}$ values were determined as the concentration of the compounds inducing death of 50% cell population.

### Acknowledgements

Peptide CSB platform, Institut Pasteur de Lille (protein HPLC analyses).

Chimie-ParisTech Laboratoire de spectrométrie de masse.

Institut Curie Protein Mass Spectrometry Laboratory.

### Supplementary data

Supplementary data associated with this article can be found, in the online version, at http://dx.doi.org/10.1016/j.bmc.2015.10.010.

### References and notes

1. Baluch, S.; Midwood, C. J.; Griffiths, J. R.; Stubbs, M.; Coombes, R. C. *Br. J. Cancer* **1991**, *63*, 901.
2. Maeda, H.; Fang, J.; Inutsuka, T.; Kitamoto, Y. *Int. Immunopharmacol.* **2003**, *3*, 319.
3. Majumdar, S.; Siahaan, T. J. *Med. Res. Rev.* **2012**, *32*, 637.
4. Flygare, J. A.; Pillow, T. H.; Aristoff, P. *Chem. Biol. Drug Des.* **2013**, *81*, 113.
5. Jain, N.; Smith, S. W.; Ghone, S.; Tomczuk, B. *Pharm. Res.* **2015**.
6. Adams, G. P.; Weiner, L. M. *Nat. Biotechnol.* **2005**, *23*, 1147.
7. Baker, M. *Nat. Biotechnol.* **2005**, *23*, 1065.
8. Carter, P. J. *Nat. Rev. Immunol.* **2006**, *6*, 343.
9. Carson, K. L. *Nat. Biotechnol.* **2005**, *23*, 1054.
10. Junutula, J. R.; Raab, H.; Clark, S.; Bhakta, S.; Leipold, D. D.; Weir, S.; Chen, Y.; Simpson, M.; Tsai, S. P.; Dennis, M. S.; Lu, Y.; Meng, Y. G.; Ng, C.; Yang, J.; Lee, C. C.; Duenas, E.; Gorrell, J.; Katta, V.; Kim, A.; McDorman, K.; Flagella, K.; Venook, R.; Ross, S.; Spencer, S. D.; Lee Wong, W.; Lowman, H. B.; Vandlen, R.; Sliwkowski, M. X.; Scheller, R. H.; Polakis, P.; Mallet, W. *Nat. Biotechnol.* **2008**, *26*, 925.
11. Doronina, S. O.; Mendelsohn, B. A.; Bovee, T. D.; Cerveny, C. G.; Alley, S. C.; Meyer, D. L.; Oflazoglu, E.; Toki, B. E.; Sanderson, R. J.; Zabinski, R. F.; Wahl, A. F.; Senter, P. D. *Bioconjugate Chem.* **2005**, *17*, 114.
12. Zhao, R. Y.; Wilhelm, S. D.; Audette, C.; Jones, G.; Leece, B. A.; Lazar, A. C.; Goldmacher, V. S.; Singh, R.; Kovtun, Y.; Widdison, W. C.; Lambert, J. M.; Chari, R. V. J. *J. Med. Chem.* **2011**, *54*, 3606.
13. Dosio, F.; Brusa, P.; Cattel, L. *Toxins* **2011**, *3*, 848.
14. Johannes, L.; Romer, W. *Nat. Rev. Microbiol.* **2010**, *8*, 105.
15. Kovbasnjuk, O.; Mourtazina, R.; Baibakov, B.; Wang, T.; Elowsky, C.; Choti, M. A.; Kane; Donowitz, M. *Proc. Natl. Acad. Sci. U.S.A.* **2005**, *102*, 19087.
16. Arab, S.; Russel, E.; Chapman, W. B.; Rosen, B.; Lingwood, C. A. *Oncol. Res.* **1997**, *9*, 553.
17. LaCasse, E. C.; Bray, M. R.; Patterson, B.; Lim, W. M.; Perampalam, S.; Radvanyi, L. G.; Keating, A.; Stewart, A. K.; Buckstein, R.; Sandhu, J. S.; Miller, N.; Banerjee, D.; Singh, D.; Belch, A. R.; Pilarski, L. M.; Gariepy, J. *Blood* **1999**, *94*, 2901.
18. Amessou, M.; Carrez, D. L.; Patin, D.; Sarr, M.; Grierson, D. S.; Croisy, A.; Tedesco, A. C.; Maillard, P.; Johannes, L. *Bioconjugate Chem.* **2008**, *19*, 532.
19. Engedal, N.; Skotland, T.; Torgersen, M. L.; Sandvig, K. *Microb. Biotechnol.* **2011**, *4*, 32.
20. Rostovtsev, V. V.; Green, L. G.; Fokin, V. V.; Sharpless, K. B. *Angew. Chem., Int. Ed.* **2002**, *41*, 2596.
21. Kolb, H. C.; Sharpless, K. B. *Drug Discovery Today* **2003**, *8*, 1128.
22. Link, A. J.; Tirrell, D. A. *J. Am. Chem. Soc.* **2003**, *125*, 11164.
23. Deiters, A.; Cropp, T. A.; Mukherji, M.; Chin, J. W.; Anderson, J. C.; Schultz, P. G. *J. Am. Chem. Soc.* **2003**, *125*, 11782.
24. Baskin, J. M.; Prescher, J. A.; Laughlin, S. T.; Agard, N. J.; Chang, P. V.; Miller, I. A.; Lo, A.; Codelli, J. A.; Bertozzi, C. R. *Proc. Natl. Acad. Sci. U.S.A.* **2007**, *104*, 16793.
25. Jewett, J. C.; Bertozzi, C. R. *Chem. Soc. Rev.* **2010**, *39*, 1272.
26. Grinda, M.; Clarhaut, J.; Renoux, B.; Tranoy-Opalinski, I.; Papot, S. *Med. Chem. Commun.* **2012**, *3*, 68.
27. Schultz, M. K.; Parameswarappa, S. G.; Pigge, F. C. *Org. Lett.* **2010**, *12*, 2398.
28. Richter, M.; Chakrabarti, A.; Ruttekolk, I. R.; Wiesner, B.; Beyermann, M.; Brock, R.; Rademann, J. *Chemistry* **2012**, *18*, 16708.
29. Lowe, A. B. *Polymer* **2014**, *55*, 5517.
30. Tantama, M.; Lin, W.-C.; Licht, S. *J. Am. Chem. Soc.* **2008**, *130*, 15766.
31. El Alaoui, A.; Schmidt, F.; Amessou, M.; Sarr, M.; Decaudin, D.; Florent, J.-C.; Johannes, L. *Angew. Chem., Int. Ed.* **2007**, *46*, 6469.
32. DeWit, M.; Gillies, E. *J. Am. Chem. Soc.* **2009**, *131*, 18327.
33. Chalker, J. M.; Lercher, L.; Rose, N. R.; Schofield, C. J.; Davis, B. G. *Angew. Chem., Int. Ed.* **2012**, *51*, 1835.
34. Satyam, A. *Bioorg. Med. Chem. Lett.* **2008**, *18*, 3196.
35. Jones, L. R.; Goun, E. A.; Shinde, R.; Rothbard, J. B.; Contag, C. H.; Wender, P. A. *J. Am. Chem. Soc.* **2006**, *128*, 6526.
36. Mallard, F.; Johannes, L. Shiga Toxin B-Subunit as a Tool to Study Retrograde Transport. In *Methods Mol. Med. Shiga Toxin Methods and Protocols*; Philpott, D., Ebel, F., Eds.; , 2003; Vol. 73, pp 209–220. Chapter 17.